2014

# Neuronal activity regulates extracellular tau in vivo

Kaoru Yamada
*Washington University School of Medicine in St. Louis*

Jerrah K. Holth
*Washington University School of Medicine in St. Louis*

Fan Liao
*Washington University School of Medicine in St. Louis*

Floy R. Stewart
*Washington University School of Medicine in St. Louis*

Thomas E. Mahan
*Washington University School of Medicine in St. Louis*

*See next page for additional authors*

# Neuronal activity regulates extracellular tau in vivo

Kaoru Yamada,[1] Jerrah K. Holth,[1] Fan Liao,[1] Floy R. Stewart,[1] Thomas E. Mahan,[1] Hong Jiang,[1] John R. Cirrito,[1] Tirth K. Patel,[1] Katja Hochgräfe,[2,3] Eva-Maria Mandelkow,[2,3] and David M. Holtzman[1]

[1]Department of Neurology, Hope Center for Neurological Disorders, Knight Alzheimer's Disease Research Center, Washington University School of Medicine, St. Louis, MO 63110
[2]DZNE (German Center for Neurodegenerative Diseases), 53175 Bonn, Germany
[3]CAESAR Research Center, 53175 Bonn, Germany

**Tau is primarily a cytoplasmic protein that stabilizes microtubules. However, it is also found in the extracellular space of the brain at appreciable concentrations. Although its presence there may be relevant to the intercellular spread of tau pathology, the cellular mechanisms regulating tau release into the extracellular space are not well understood. To test this in the context of neuronal networks in vivo, we used in vivo microdialysis. Increasing neuronal activity rapidly increased the steady-state levels of extracellular tau in vivo. Importantly, presynaptic glutamate release is sufficient to drive tau release. Although tau release occurred within hours in response to neuronal activity, the elimination rate of tau from the extracellular compartment and the brain is slow (half-life of ∼11 d). The in vivo results provide one mechanism underlying neuronal tau release and may link trans-synaptic spread of tau pathology with synaptic activity itself.**

CORRESPONDENCE
David M. Holtzman:
holtzman@neuro.wustl.edu

Abbreviations used: AD, Alzheimer's disease; ISF, interstitial fluid; LDH, lactose dehydrogenase; NFT, neurofibrillary tangle; NMDA, *N*-Methyl-D-aspartic acid; PTX, picrotoxin; TTX, tetrodotoxin.

Tau is a major component of neurofibrillary tangles (NFTs) in Alzheimer's disease (AD) and other disorders known as tauopathies. The burden and distribution of NFTs correlate well with cognitive decline in AD (Arriagada et al., 1992; Bancher et al., 1993). In AD, NFTs are prominent early in entorhinal cortex and later appear in anatomically connected brain regions (Braak and Braak, 1995). Cell to cell transmission is one hypothesis accounting for this phenomenon (Mohamed et al., 2013). Previous studies suggest that certain forms of tau released into the extracellular space can enter cells and induce further tau aggregation (Clavaguera et al., 2009; Frost et al., 2009; Guo and Lee, 2011; Kfoury et al., 2012; Iba et al., 2013). Tau pathology appears to spread trans-synaptically from entorhinal cortex to hippocampus before marked neurodegeneration (de Calignon et al., 2012; Harris et al., 2012; Liu et al., 2012). Studies suggest that tau can be secreted into the extracellular space from neurons independently from cell death (Chai et al., 2012; Karch et al., 2012). In addition, the elevation of tau in cerebrospinal fluid is associated with AD and is linked to Aβ deposition (Jack et al., 2013; Maia et al., 2013). Despite the fact that extracellular tau may initiate synaptic spread of tau pathology, the mechanisms regulating neuronal release of extracellular tau are not fully understood.

We hypothesized that neuronal activity regulates release of tau from neurons. To test this idea in the setting of mature neuronal networks, we used in vivo microdialysis and analyzed the kinetics of release and clearance of extracellular tau in brain interstitial fluid (ISF).

## RESULTS AND DISCUSSION

### Increasing neuronal activity increases ISF tau in vivo

The technique of in vivo microdialysis enables the hourly measurement of endogenous ISF tau from wild-type mice. During microdialysis, mice are awake and freely moving, allowing for the assessment of mechanisms regulating ISF tau in the context of normally functioning neuronal networks. We reasoned that if neuronal activity is a major regulator of tau release into the ISF, altered activity would result in a change



The Rockefeller University Press $30.00
J. Exp. Med. 2014 Vol. 211 No. 3 387-393
www.jem.org/cgi/doi/10.1084/jem.20131685

in the level of preexisting extracellular tau in vivo. After baseline tau measurement, hippocampal neurons were locally depolarized by briefly exposing them to high $K^+$ perfusion buffer via reverse microdialysis. Consistent with an elevation in neuronal activity, depolarization rapidly decreased glucose by 46% (Fig. 1 A) and increased lactate by 171% (Fig. 1 B) in ISF. Lactate and glucose rapidly returned to baseline levels after wash out. ISF tau increased by 68% from baseline in response to high $K^+$ (Fig. 1 C) in the first hour and continued to increase by up to 152% during the wash out period. Once peak tau concentrations were reached, ISF tau returned to baseline levels over hours. To determine the levels of neuronal activity in response to high $K^+$, we used intrahippocampal EEG recording to assess extracellular field potentials during high $K^+$ depolarization. The infusion of high $K^+$ resulted in EEG bursting activity (Fig. 1 D).

To stimulate neurons at lower frequency and avoid any potential cell injury or death caused by higher activity such as is found in prolonged seizures, picrotoxin (PTX), a noncompetitive $GABA_A$ receptor antagonist was locally and continuously infused in hippocampus via reverse microdialysis at relatively low doses. In contrast to EEG bursting activity caused by high $K^+$, the low dose of PTX used in this study only produced occasional spikes, as assessed by EEG, but no epileptiform activity or seizures (Fig. 2 A). This is similar to what we have observed previously (Cirrito et al., 2008; Bero et al., 2011). PTX decreased glucose by 33% and increased lactate by 342% (Fig. 2, B and C) consistent with increased neuronal activity. PTX also rapidly increased ISF tau by 149% within hours (Fig. 2 D). In contrast to the brief depolarization by high $K^+$, the increase of ISF tau was maintained while neurons were activated by infusion of PTX. PTX did not alter tau levels in hippocampal tissue lysates, further confirming that increase of ISF tau is due to the release from neurons and not due to an increased level of total tau proteins inside cells (Fig. 2 E).

To further assess whether the treatments we administered to increase neuronal activity were not causing cellular damage or death, further assays were performed. Neuronal damage, including loss of membrane integrity, causes nonspecific release of intracytoplasmic proteins such as lactose dehydrogenase (LDH). Thus, we measured LDH activity in ISF of P301S human tau transgenic mice in the presence of PTX administered by reverse microdialysis. PTX treatment resulted in a two- to threefold increase in ISF human tau in P301S human tau transgenic mice (Fig. 2 F), similar to the increase seen in mouse tau in wild-type mice. However, PTX did not increase LDH activity in ISF (Fig. 2, G and H). The administration of pilocarpine is known to cause seizures and excitotoxic injury in brain. Systemic administration of pilocarpine resulted in seizure activity within 30 min in all mice. It also resulted in an increase of ISF tau by 10–15-fold from baseline (Fig. 2 F). Unlike PTX, pilocarpine significantly increased LDH activity, confirming that excitotoxic injury releases cytoplasmic proteins nonspecifically (Fig. 2, G and H). Pilocarpine administration rapidly induced abnormal activation of neurons, as is evident by seizure phenotypes observed within 30 min in all mice. Nevertheless, the release of LDH by pilocarpine was only observed much later after seizures began (~7.5 h later; Fig. 2 G). These findings strongly suggest that nonspecific release of cytoplasmic proteins by excitotoxic brain injury is a much slower process than the activity-dependent release of tau in ISF. Consistent with this data, pilocarpine, but not PTX, increased degenerating neurons stained by Fluoro-Jade C (unpublished data). Collectively, the data strongly suggests that the increase of ISF tau by PTX is due to enhanced neuronal activity and not due to neuronal injury or death caused by excitotoxic injury.

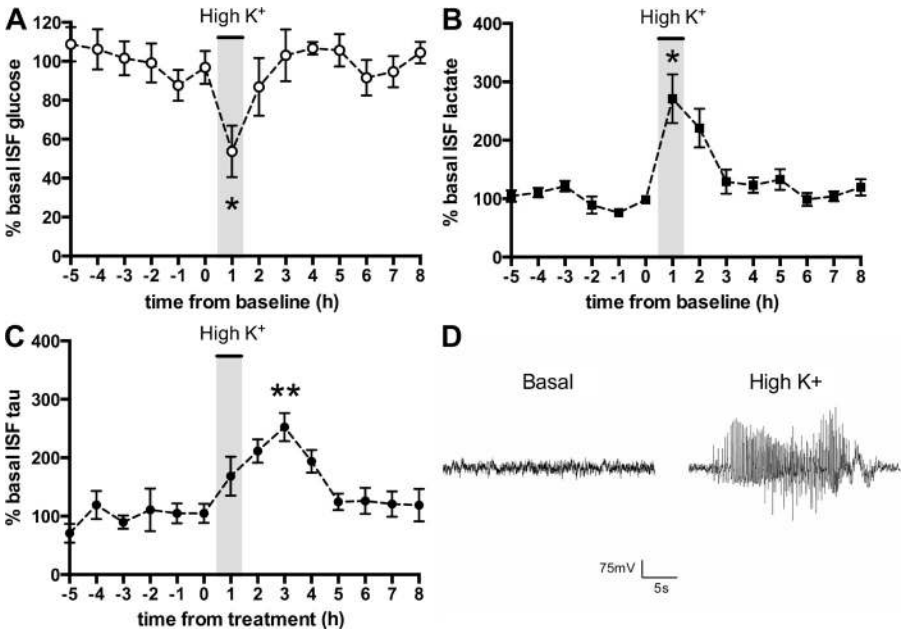


**Figure 1. Depolarization increases tau in ISF.** (A–C) Microdialysis experiments were performed in hippocampi of wild-type mice. After baseline collection, the regular perfusion buffer was switched to high $K^+$ perfusion buffer (administration indicated by gray box). After 1 h, the buffer was switched back to normal perfusion buffer (wash out) and ISF collection was continued. Glucose (A), lactate (B), and tau (C) in ISF were measured. ($n = 5$; *, $P < 0.05$; **, $P < 0.01$). For mice studied in A–C, each mouse was investigated independently. Any treatment effects were compared with baseline values within each mouse. Error bars represent SEM. (D) Representative EEG trace from one of three mice during depolarization with high $K^+$ perfusion buffer.

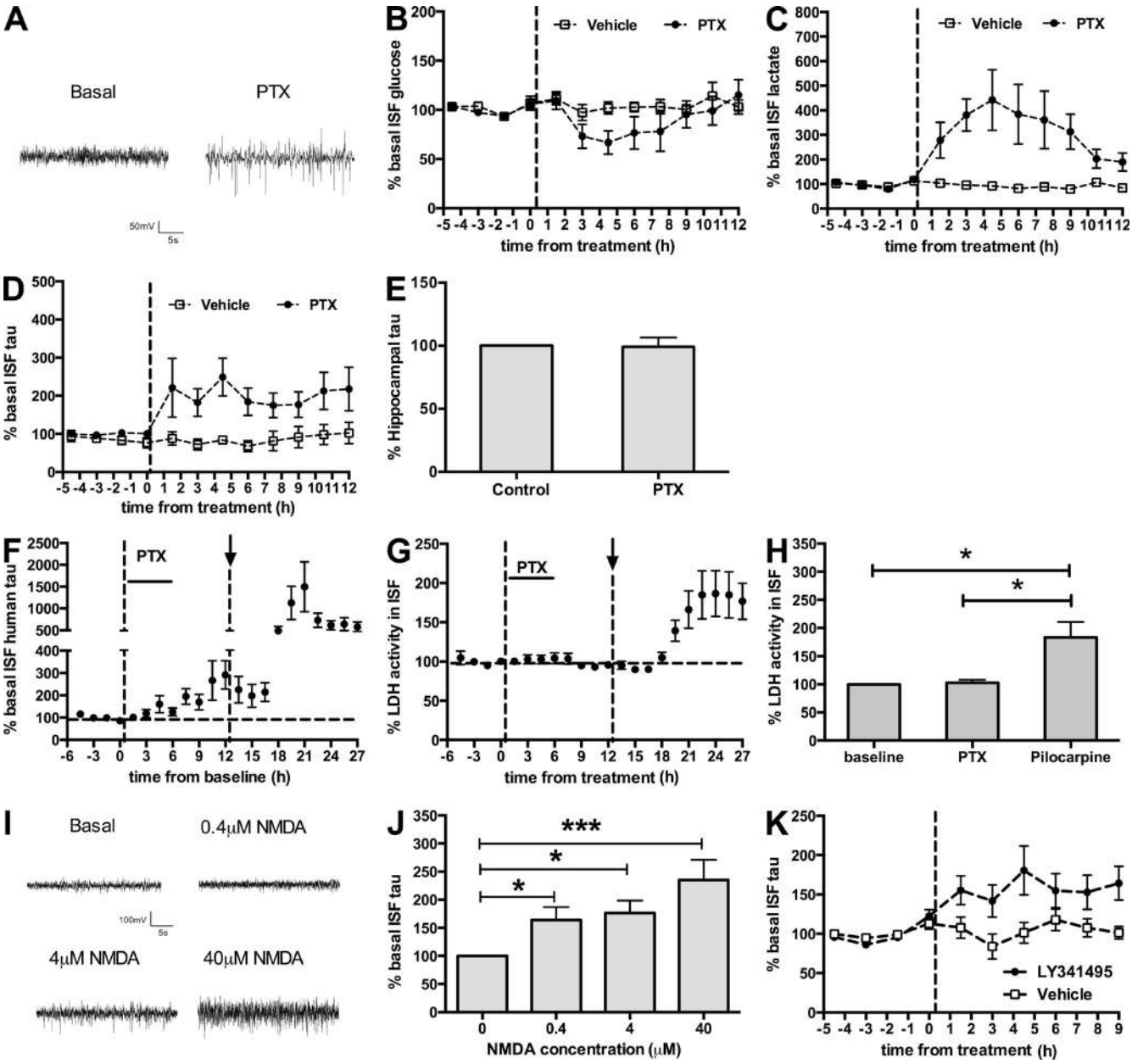


**Figure 2. Neuronal activity and synaptic activity increase tau in ISF.** (A) Representative EEG trace from one of three mice during depolarization with high $K^+$ perfusion buffer. 25 µM PTX was delivered directly into the hippocampus of wild-type mice via reverse microdialysis (indicated by dashed line). (B–D) Glucose (B), lactate (C), and tau (D) in ISF was measured ($n$ = 6/group). (E) Hippocampal tissue tau levels after PTX reverse microdialysis ($n$ = 6/group). (F and G) 25 µM PTX was delivered directly into the hippocampus of P301S human tau transgenic mice via reverse microdialysis for 6 h ($n$ = 5). After 6-h washout, the mice were given an i.p. injection of 325 mg/kg pilocarpine hydrochloride (indicated by arrows). Human tau (F) and LDH (G) activity in ISF was measured. The mean LDH activity was compared between groups (H; *, $P < 0.05$). (I) Representative EEG trace from one of three mice during various doses of NMDA infusion. (J) The effects of various doses of NMDA delivered by reverse microdialysis on ISF tau was measured ($n$ = 6; *, $P < 0.05$; ***, $P < 0.001$). (K) The effects of the highly selective mGluR2/3 antagonist LY341495 (administered by reverse microdialysis) on ISF tau was measured ($n$ = 6 for LY341495, $n$ = 7 for vehicle). Error bars represent SEM. For mice studied in B–D, F–H, and J–K, each mouse was investigated independently. Any treatment effects were compared with baseline values within each mouse.

To examine how ISF tau can be regulated by the increasing neuronal activity to different degrees, we administered increasing doses of *N*-Methyl-D-aspartic acid (NMDA) in the hippocampus. NMDA administered via reverse microdialysis at doses of 1–40 µM has dose-dependent effects on excitatory neuronal activity—measured by EEG—without causing cell death or neurodegeneration (Fig. 2 I;Verges et al., 2011). Consistent with the EEG data, NMDA resulted in a dose-dependent increase of ISF tau (Fig. 2 J), suggesting that the degree of neuronal activity can determine ISF tau levels. Given that

the $EC_{50}$ of NMDA receptors is 35 µM in vitro, NMDA concentrations of 0.4–4 µM delivered via reverse microdialysis in this study should activate only a small percentage of the receptors (Verges et al., 2011). Nevertheless it is sufficient to drive an ∼70% increase of ISF tau, suggesting that excitatory neuronal activity has a significant impact on ISF tau.

Metabotropic glutamate receptors 2/3 (mGluR2/3) are expressed at the presynaptic terminal and regulate glutamate release. The inhibition of these receptors enhances glutamate release from the presynaptic terminals (Cirrito et al., 2008). To specifically ask whether the presynaptic excitatory neuronal activity modulates ISF tau, LY 341495, a highly selective mGluR2/3 antagonist was infused into the hippocampus via reverse microdialysis and ISF tau was simultaneously measured. LY 341495 caused a rapid increase of ISF tau by 80% (Fig. 2 K). This data links presynaptic excitatory neuronal activity with tau release. Collectively, these data strongly suggest that excitatory neuronal activity can rapidly alter the steady-state levels of extracellular tau levels in vivo.

### The effect of TTX on ISF tau levels in vivo

We next asked whether inhibiting neuronal activity alters ISF tau. To this end, we infused the voltage-gated sodium channel blocker tetrodotoxin (TTX). Surprisingly, TTX did not cause a decrease of basal ISF tau within the window of microdialysis (Fig. 3 A). In contrast, TTX rapidly decreased endogenous Aβ in the ISF by 35% (Fig. 3 B), as we previously reported (Cirrito et al., 2005). Confirming that TTX does have an effect on tau release, pre-administration of TTX blocked the NMDA-induced increase in ISF tau (Fig. 3 C).

### The in vivo turnover rate of tau

To try to explain the lack of acute responsiveness of basal ISF tau to blocking neuronal activity, we note that the balance between cellular release and clearance determines the steady-state levels of proteins measured by microdialysis. Inhibiting synaptic activity reduces ISF Aβ production and release. Reduced Aβ release can be visualized quickly, as the in vivo half-life of Aβ is ∼2 h (Cirrito et al., 2005), leading to the rapid elimination of Aβ by clearance mechanisms. Unlike Aβ, tau is known as a very stable protein (Price et al., 2010). This raised the possibility that slow turnover might prevent the ability to see an effect of TTX on inhibition of basal ISF tau release over hours.

To examine the clearance of soluble tau in vivo, the turnover rate of tau was kinetically analyzed using transgenic mice, which express a non-aggregating form of human tau (anti-aggregant mice: 2N4R-tau with ΔK280/PP mutations). The expression of human tau in these mice can be quickly switched off by doxycycline (Eckermann et al., 2007). These mice do not develop tau pathology, allowing us to examine the clearance of soluble tau without the influence of tau aggregates (Van der Jeugd et al., 2012; Hochgräfe and Mandelkow, 2013). To be able to analyze the elimination of ISF tau chronically for up to 18 d by microdialysis, mice were divided into five groups where human tau expression was switched off for the predetermined length of time. One cohort of mice was not exposed to doxycycline to determine the initial human tau levels before tau switch-off. In vivo microdialysis was performed in all groups and levels of ISF tau were assessed over 2 d in each mouse. ISF human tau levels were determined by ELISA. The absolute ISF human tau levels after switch-off were normalized to the level of ISF human tau in the mice without switch-off. Soluble human tau in the hippocampus where ISF tau was collected was also analyzed at the end of microdialysis.

Switch-off specifically decreased human tau in hippocampal lysates in a time-dependent manner without changing endogenous murine tau levels, confirming the specificity of switch-off. ISF human tau was also decreased over time, whereas lactate levels did not decrease (Fig. 4, A and B). The elimination of tau followed first-order kinetics and the half-life was calculated as 11.1 d for soluble tau in hippocampus and 10.9 d for ISF tau, respectively. The clearance rate of tau in hippocampal tissue was comparable to a previous report assessing total tissue tau (Price et al., 2010; Fig. 4, C and D).

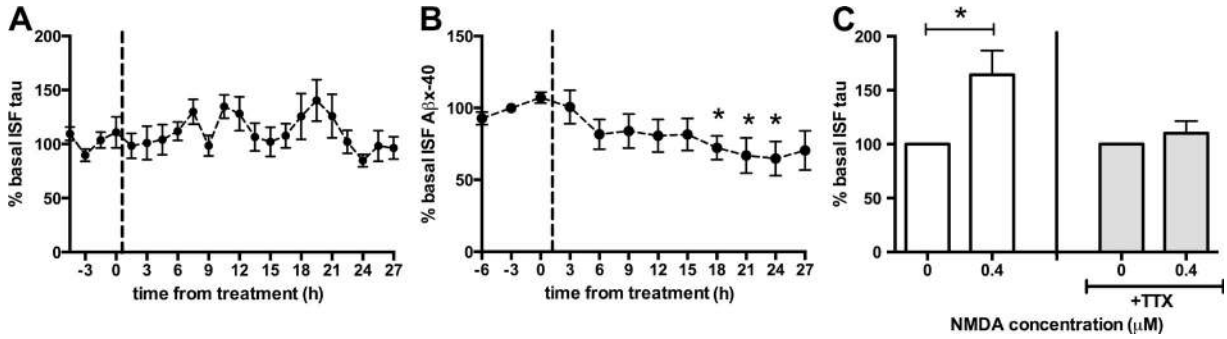


**Figure 3. TTX does not cause an acute decrease of ISF tau.** After baseline ISF tau collection, 5 µM TTX was delivered via reverse microdialysis (indicated by dashed line). The effect of TTX on ISF tau (A; $n = 10$) and ISF endogenous Aβx-40 (B; $n = 7$; *, $P < 0.05$) is shown. The effect of preadministration of TTX on ISF tau in the presence of 0.4 µM NMDA (C; $n = 6–7$ per group; *, $P < 0.05$) is also shown. Both TTX and NMDA were administered by reverse microdialysis in C. Error bars represent SEM. Each mouse studied in A–C was investigated independently. Any treatment effects were compared with baseline values within each mouse.

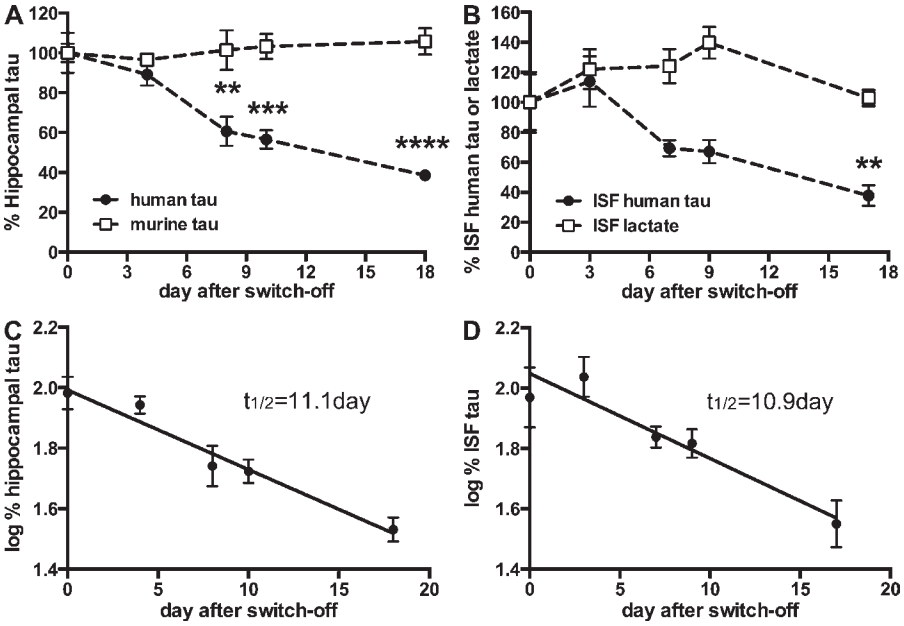


**Figure 4. The turnover rate of tau in hippocampus and ISF is low.** Human tau expression in anti-aggregant mice was switched off for the indicated lengths of time by doxycycline, and human tau (black circle) and murine tau (white square) levels in hippocampus were measured by ELISA (A; $n$ = 5–7/group/time point; **, $P < 0.01$; ***, $P < 0.001$; ****, $P < 0.0001$). Human tau (black circle) and lactate (white square) in ISF after switch-off were measured by ELISA (B; $n$ = 4–5/group/time point; **, $P < 0.01$). The plot of the common logarithm of percent tau in hippocampal lysates or ISF versus time was linear in both groups studied. The slope from the linear regressions from log (% tau) versus time was used to calculate the half-life ($t_{1/2}$) of elimination for tau from hippocampus (C) and ISF (D). Each mouse studied in A–D was investigated independently. Any treatment effects were compared with baseline values obtained from mice studied at time zero. Error bars represent SEM.

This observation suggests that extracellular, ISF tau has a much longer in vivo turnover rate than Aβ. Thus, even if a substance such as TTX decreased endogenous tau release, it would be expected to take several days to see such a change.

In summary, our present study describes a mechanistic link between neuronal activity and extracellular tau in vivo. In this context, we note a very recent in vitro study using primary cultured neurons (Pooler et al., 2013) in which neuronal activity is also linked to increased tau release. Importantly, we found that neuronal activity rapidly alters the steady-state levels of preexisting ISF tau in vivo. Furthermore, presynaptic glutamate release by mGluR2/3 antagonist LY 341495 is sufficient to increase ISF tau, suggesting that presynaptic excitatory neuronal activity is linked to tau release. Although neuronal activity increases tau release within hours, tau clearance, which is distinct from diffusion to adjacent areas of the brain with lower tau, requires many days. This slow turnover will delay the elimination of extracellular tau and, as a consequence, it may affect its aggregation and synaptic transmission of tau pathology. Intriguingly, not only tau but also many other intraneuronal proteins have been identified in the extracellular space of brains, although the mechanism of release of these cytoplasmic proteins remains unknown (Lee et al., 2005). Among them are proteins such as α-synuclein, which contributes to cell to cell transmission of Parkinson's disease pathology (Luk et al., 2012). The mechanism we report here may have broader implications to elucidate mechanisms of release and prion-like spread of intracellular proteins involved in neurodegeneration.

## MATERIALS AND METHODS

**Compounds.** PTX, TTX, NMDA, and pilocarpine were obtained from Sigma-Aldrich. LY341495 was obtained from Abcam.

**Animals.** All animal studies performed were reviewed and approved by the Animal Studies Committee at Washington University. 3–5-mo-old male and female P301S human tau transgenic mice and wild-type littermates on B6C3 background were used for microdialysis studies. Regulatable transgenic mice expressing anti-aggregant human full-length tau mice (Tau 2N4R with mutations deltaK280/PP) on C57BL/6 background were generated as previously described (Eckermann et al., 2007). Mice were screened for the expression of exogenous tau by in vivo bioluminescence imaging of luciferase assay (Hochgräfe and Mandelkow, 2013). Individuals with signal intensities $>10^7$ p/s were selected for switch-off experiments (Van der Jeugd et al., 2012).

**In vivo microdialysis.** In vivo microdialysis experiments to assess brain ISF tau levels from awake and freely moving mice were developed with modifications of our previously described method (Yamada et al., 2011). A guide cannula (Eicom microdialysis) was stereotactically implanted in the left hippocampus under isoflurane anesthesia, and cemented. After implantation of the cannula and dummy probes (Eicom microdialysis), mice were habituated to microdialysis cages for one more day. After this recovery period, a 2-mm 1,000-kD cut-off AtmosLM microdialysis probe (Eicom) was inserted through the guide cannula. A probe was connected to a microdialysis peristaltic pump with two channels (MAB20; SciPro), which was operated in a push-pull mode. As a perfusion buffer, 25% human albumin solution (Gemini Bio Inc.) was diluted to 4% with artificial CSF (aCSF; 1.3 mM $CaCl_2$, 1.2 mM $MgSO_4$, 3 mM KCl, 0.4 mM $KH_2PO_4$, 25 mM $NaHCO_3$, and 122 mM NaCl, pH 7.35) on the day of use and filtered through a 0.1-µm membrane. For 100 mM high $K^+$ stimulation, 97 mM KCl in aCSF was substituted for an equal amount of NaCl. Normal perfusion buffer was switched to high $K^+$ perfusion buffer for 1 h. Before microdialysis sample collection, a pump was run at the maximum flow rate for at least 1 h. For ISF collection from wild-type mice, 1 µl/min was used. For ISF human tau collection from transgenic mice expressing anti-aggregant human full-length tau (deltaK280/PP), 0.5 µl/min was used. To avoid tissue damage, the experimental window was set from 6 to 48 h after probe implantation. We confirmed that within this timeframe, ISF tau and Aβx-40 concentrations remain stable under constant light conditions. ISF samples were collected in a refrigerated fraction collector (SciPro) and analyzed by ELISA. 25 µM PTX, 5 µM TTX, 0.4–40 µM NMDA, and 100 µM LY341495 were delivered into ISF via reverse microdialysis. For NMDA reverse microdialysis, each dose of NMDA was administrated for 5 h in ascending fashion. To assess the effect of TTX on the increase of ISF tau by NMDA, 5 µM TTX was delivered by reverse microdialysis for 12 h, followed by co-infusion of 0.4 µM NMDA and 5 µM TTX for 12 h.

**EEG recording.** Electrical activity was recorded in the hippocampus surrounding the microdialysis probe similar to Cirrito et al. (2008). In brief, bipolar recording electrodes (Teflon-coated, stainless steel wire, 0.0055-in coated OD; A-M Systems) were attached to the shaft of the microdialysis guide cannula (BR-style; Bioanalytical) with Super-Fast Epoxy Resin (Elmer's). Electrodes extended ∼1 mm from the tip of the guide, so that the electrode tip was located at the center of the 2-mm microdialysis membrane. EEG activity was assessed using a P511K A.C. pre-amplifier (Grass Instruments), digitized with a DigiData 1440 Data Acquisition System (Molecular Devices), and recorded digitally using Axoscope 10.2. Compounds were administered directly to the brain via reverse microdialysis at a flow rate of 1 µl/min.

**Switch-off experiments.** 16–17-mo-old transgenic mice expressing anti-aggregant human full-length tau (deltaK280/PP) were randomly divided into five groups. One cohort of mice was not exposed to doxycycline-containing food pellets (200 mg/kg; Bio-serv) and ISF was collected for 48 h (0 day groups). Other cohorts of mice received doxycycline-containing food pellets for 2, 6, 8, or 16 d, respectively before microdialysis. On day 2, 6, 8, or 16, in vivo microdialysis was started and ISF samples were collected for 48 h. During microdialysis, mice were given doxycycline-containing food pellets. Brains were collected on day 4, 8, 10, or 18, respectively, at the end of microdialysis experiments. Hippocampus where microdialysis probes were inserted was used to determine intracellular human tau levels in hippocampus. Percentages of brain human tau, ISF human tau, and ISF lactate were normalized by the mean concentration in 0 day groups.

**Pilocarpine injection.** Mice received a low dose of methyl scopolamine (1 mg/kg) to reduce peripheral cholinergic effects. After 30 min, mice were given i.p. injection of 325 mg/kg pilocarpine hydrochloride. All animals injected with pilocarpine displayed motor seizure phenotype. 15 min after pilocarpine injection, the mice were injected with pentobarbital to terminate seizures.

**Tau ELISA.** The tau concentration in media of brain slice culture and ISF of wild-type mice was analyzed in a tau sandwich ELISA with Tau-5 as a coating antibody (gift from L. Binder, Northwestern University, Evanston, IL) and biotinylated BT-2 (Thermo Fisher Scientific) as a detection antibody as previously described (Yamada et al., 2011). Human tau in ISF and brains was measured by a human tau-specific sandwich ELISA with Tau-5 as a coating antibody and biotinylated human specific HT-7 (Thermo Fisher Scientific) as a detection antibody. Murine endogenous tau in brains was measured by a sandwich ELISA with HJ9.2 as a coating antibody and biotinylated tau antibodies (HJ8.7) as a detection antibody. HJ8.7 and HJ9.2 are in-house mouse monoclonal antibodies that recognize the N-terminal domain of tau (epitope of HJ8.7: residues 118–122; epitope of HJ9.2: residues 4–8). The human tau levels in samples were determined by subtracting background signals from wild type in Tau-5/HT7 ELISA.

**Aβx-40 ELISA.** Aβx-40 ELISA was done as previously described (Cirrito et al., 2008). Background determined by signal from the microdialysis perfusion buffer was subtracted.

**Glucose and lactate measurements.** Glucose and lactate concentration in ISF and media was determined by YSI2700 biochemistry analyzer (YSI Life Sciences). Glucose was used as a marker of substrate utilization, and lactate was used as a marker of neuronal activity (Bero et al., 2011).

**Brain extraction.** Mice were perfused with chilled PBS-heparin. Brains were dissected for biochemical analysis and kept at −80°C until analyzed. To analyze tau after PTX infusion, left (exposed to PTX by reverse microdialysis) and right hippocampi were dissected at 4.5 h after PTX infusion where both ISF lactate and tau showed the highest increases from baseline. Tau in hippocampal lysates was determined by Tau-5/BT2 ELISA. Contralateral hippocampus (right) was used as a control. In switch-off experiments, hippocampus was weighed and homogenized in RAB buffer (100 mM MES, 1 mM EDTA, 0.5 mM $MgSO_4$, 750 mM NaCl, 20 mM NaF, and 1 mM $Na_3VO_4$, supplemented by protease inhibitors [Complete; Roche] and phosphatase inhibitors [PhosSTOP; Roche]). The samples were centrifuged at 50,000 *g* for 20 min at 4°C. The supernatants were collected as RAB soluble fractions. The pellets were further homogenized by RIPA buffer (150 mm NaCl, 50 mm Tris, 0.5% deoxycholic acid, 1% Triton X-100, and 0.5% SDS–25 mm EDTA, pH 8.0, supplemented by protease inhibitor [Complete; Roche] and phosphatase inhibitor [PhosSTOP; Roche]). Total tau in both RAB and RIPA soluble fractions were combined and used as brain soluble tau.

**The calculation of half-life.** The elimination of tau in brain lysates and ISF followed first-order kinetics. Thus $t_{1/2}$ for tau was calculated with the slope, k′, of the linear regression ($t_{1/2} = 0.693/k$, where $k = 2.303k'$) as we previously reported (Castellano et al., 2011).

**LDH assay.** LDH activity in ISF was determined by Lactate Dehydrogenase Activity Assay kit (Sigma-Aldrich). The final measurement [(A450)final] for calculating the enzyme activity was normalized by the baseline activities. After normalization, mean LDH activity during the 6-h PTX treatment and in the last 6-h pilocarpine treatment were compared with baseline.

**Statistical analysis.** Data in figures represent mean ± SEM. All statistical analysis was performed using Prism (version 5.04 for Windows; GraphPad Software). Analysis of the effects of drugs compared with vehicle control was done by two-way ANOVA with repeated measures. The comparison between baseline and post-treatment was done by paired Student's *t* test. The comparison of multiple groups was done by one-way ANOVA. Values were considered significant if $P < 0.05$.

This work was supported by Japan Society for the promotion of Science (K. Yamada) and the Tau consortium (D.M. Holtzman and E.-M. Mandelkow).

The authors declare no competing financial interests.

**Submitted: 11 August 2013**
**Accepted: 27 January 2014**

## REFERENCES

Arriagada, P.V., J.H. Growdon, E.T. Hedley-Whyte, and B.T. Hyman. 1992. Neurofibrillary tangles but not senile plaques parallel duration and severity of Alzheimer's disease. *Neurology*. 42:631–639. http://dx.doi.org/10.1212/WNL.42.3.631

Bancher, C., H. Braak, P. Fischer, and K.A. Jellinger. 1993. Neuropathological staging of Alzheimer lesions and intellectual status in Alzheimer's and Parkinson's disease patients. *Neurosci. Lett.* 162:179–182. http://dx.doi.org/10.1016/0304-3940(93)90590-H

Bero, A.W., P. Yan, J.H. Roh, J.R. Cirrito, F.R. Stewart, M.E. Raichle, J.-M. Lee, and D.M. Holtzman. 2011. Neuronal activity regulates the regional vulnerability to amyloid-β deposition. *Nat. Neurosci.* 14:750–756. http://dx.doi.org/10.1038/nn.2801

Braak, H., and E. Braak. 1995. Staging of Alzheimer's disease-related neurofibrillary changes. *Neurobiol. Aging*. 16:271–278. http://dx.doi.org/10.1016/0197-4580(95)00021-6

Castellano, J.M., J. Kim, F.R. Stewart, H. Jiang, R.B. DeMattos, B.W. Patterson, A.M. Fagan, J.C. Morris, K.G. Mawuenyega, C. Cruchaga, et al. 2011. Human apoE isoforms differentially regulate brain amyloid-β peptide clearance. *Sci. Transl. Med.* 3:89ra57.

Chai, X., J.L. Dage, and M. Citron. 2012. Constitutive secretion of tau protein by an unconventional mechanism. *Neurobiol. Dis.* 48:356–366. http://dx.doi.org/10.1016/j.nbd.2012.05.021

Cirrito, J.R., K.A. Yamada, M.B. Finn, R.S. Sloviter, K.R. Bales, P.C. May, D.D. Schoepp, S.M. Paul, S. Mennerick, and D.M. Holtzman. 2005. Synaptic activity regulates interstitial fluid amyloid-β levels in vivo. *Neuron*. 48:913–922. http://dx.doi.org/10.1016/j.neuron.2005.10.028

Cirrito, J.R., J.-E. Kang, J. Lee, F.R. Stewart, D.K. Verges, L.M. Silverio, G. Bu, S. Mennerick, and D.M. Holtzman. 2008. Endocytosis is required for synaptic activity-dependent release of amyloid-β in vivo. *Neuron*. 58:42–51. http://dx.doi.org/10.1016/j.neuron.2008.02.003

Clavaguera, F., T. Bolmont, R.A. Crowther, D. Abramowski, S. Frank, A. Probst, G. Fraser, A.K. Stalder, M. Beibel, M. Staufenbiel, et al. 2009. Transmission and spreading of tauopathy in transgenic mouse brain. *Nat. Cell Biol.* 11:909–913. http://dx.doi.org/10.1038/ncb1901

de Calignon, A., M. Polydoro, M. Suárez-Calvet, C. William, D.H. Adamowicz, K.J. Kopeikina, R. Pitstick, N. Sahara, K.H. Ashe, G.A. Carlson, et al. 2012. Propagation of tau pathology in a model of early Alzheimer's disease. *Neuron.* 73:685–697. http://dx.doi.org/10.1016/j.neuron.2011.11.033

Eckermann, K., M.-M. Mocanu, I. Khlistunova, J. Biernat, A. Nissen, A. Hofmann, K. Schönig, H. Bujard, A. Haemisch, E. Mandelkow, et al. 2007. The β-propensity of Tau determines aggregation and synaptic loss in inducible mouse models of tauopathy. *J. Biol. Chem.* 282:31755–31765. http://dx.doi.org/10.1074/jbc.M705282200

Frost, B., R.L. Jacks, and M.I. Diamond. 2009. Propagation of tau misfolding from the outside to the inside of a cell. *J. Biol. Chem.* 284:12845–12852. http://dx.doi.org/10.1074/jbc.M808759200

Guo, J.L., and V.M.-Y. Lee. 2011. Seeding of normal Tau by pathological Tau conformers drives pathogenesis of Alzheimer-like tangles. *J. Biol. Chem.* 286:15317–15331. http://dx.doi.org/10.1074/jbc.M110.209296

Harris, J.A., A. Koyama, S. Maeda, K. Ho, N. Devidze, D.B. Dubal, G.-Q. Yu, E. Masliah, and L. Mucke. 2012. Human P301L-mutant tau expression in mouse entorhinal-hippocampal network causes tau aggregation and presynaptic pathology but no cognitive deficits. *PLoS ONE.* 7:e45881. http://dx.doi.org/10.1371/journal.pone.0045881

Hochgräfe, K., and E.-M. Mandelkow. 2013. Making the brain glow: in vivo bioluminescence imaging to study neurodegeneration. *Mol. Neurobiol.* 47:868–882. http://dx.doi.org/10.1007/s12035-012-8379-1

Iba, M., J.L. Guo, J.D. McBride, B. Zhang, J.Q. Trojanowski, and V.M.-Y. Lee. 2013. Synthetic tau fibrils mediate transmission of neurofibrillary tangles in a transgenic mouse model of Alzheimer's-like tauopathy. *J. Neurosci.* 33:1024–1037. http://dx.doi.org/10.1523/JNEUROSCI.2642-12.2013

Jack, C.R. Jr., D.S. Knopman, W.J. Jagust, R.C. Petersen, M.W. Weiner, P.S. Aisen, L.M. Shaw, P. Vemuri, H.J. Wiste, S.D. Weigand, et al. 2013. Tracking pathophysiological processes in Alzheimer's disease: an updated hypothetical model of dynamic biomarkers. *Lancet Neurol.* 12:207–216. http://dx.doi.org/10.1016/S1474-4422(12)70291-0

Karch, C.M., A.T. Jeng, and A.M. Goate. 2012. Extracellular Tau levels are influenced by variability in Tau that is associated with tauopathies. *J. Biol. Chem.* 287:42751–42762. http://dx.doi.org/10.1074/jbc.M112.380642

Kfoury, N., B.B. Holmes, H. Jiang, D.M. Holtzman, and M.I. Diamond. 2012. Trans-cellular propagation of Tau aggregation by fibrillar species. *J. Biol. Chem.* 287:19440–19451. http://dx.doi.org/10.1074/jbc.M112.346072

Lee, H.-J., S. Patel, and S.-J. Lee. 2005. Intravesicular localization and exocytosis of α-synuclein and its aggregates. *J. Neurosci.* 25:6016–6024. http://dx.doi.org/10.1523/JNEUROSCI.0692-05.2005

Liu, L., V. Drouet, J.W. Wu, M.P. Witter, S.A. Small, C. Clelland, and K. Duff. 2012. Trans-synaptic spread of tau pathology in vivo. *PLoS ONE.* 7:e31302. http://dx.doi.org/10.1371/journal.pone.0031302

Luk, K.C., V. Kehm, J. Carroll, B. Zhang, P. O'Brien, J.Q. Trojanowski, and V.M.-Y. Lee. 2012. Pathological α-synuclein transmission initiates Parkinson-like neurodegeneration in nontransgenic mice. *Science.* 338:949–953. http://dx.doi.org/10.1126/science.1227157

Maia, L.F., S.A. Kaeser, J. Reichwald, M. Hruscha, P. Martus, M. Staufenbiel, and M. Jucker. 2013. Changes in amyloid-β and Tau in the cerebrospinal fluid of transgenic mice overexpressing amyloid precursor protein. *Sci. Transl. Med.* 5:re2.

Mohamed, N.-V., T. Herrou, V. Plouffe, N. Piperno, and N. Leclerc. 2013. Spreading of tau pathology in Alzheimer's disease by cell-to-cell transmission. *Eur. J. Neurosci.* 37:1939–1948. http://dx.doi.org/10.1111/ejn.12229

Pooler, A.M., E.C. Phillips, D.H.W. Lau, W. Noble, and D.P. Hanger. 2013. Physiological release of endogenous tau is stimulated by neuronal activity. *EMBO Rep.* 14:389–394. http://dx.doi.org/10.1038/embor.2013.15

Price, J.C., S. Guan, A. Burlingame, S.B. Prusiner, and S. Ghaemmaghami. 2010. Analysis of proteome dynamics in the mouse brain. *Proc. Natl. Acad. Sci. USA.* 107:14508–14513. http://dx.doi.org/10.1073/pnas.1006551107

Van der Jeugd, A., K. Hochgräfe, T. Ahmed, J.M. Decker, A. Sydow, A. Hofmann, D. Wu, L. Messing, D. Balschun, R. D'Hooge, and E.-M. Mandelkow. 2012. Cognitive defects are reversible in inducible mice expressing pro-aggregant full-length human Tau. *Acta Neuropathol.* 123:787–805. http://dx.doi.org/10.1007/s00401-012-0987-3

Verges, D.K., J.L. Restivo, W.D. Goebel, D.M. Holtzman, and J.R. Cirrito. 2011. Opposing synaptic regulation of amyloid-β metabolism by NMDA receptors in vivo. *J. Neurosci.* 31:11328–11337. http://dx.doi.org/10.1523/JNEUROSCI.0607-11.2011

Yamada, K., J.R. Cirrito, F.R. Stewart, H. Jiang, M.B. Finn, B.B. Holmes, L.I. Binder, E.-M. Mandelkow, M.I. Diamond, V.M.-Y. Lee, and D.M. Holtzman. 2011. In vivo microdialysis reveals age-dependent decrease of brain interstitial fluid tau levels in P301S human tau transgenic mice. *J. Neurosci.* 31:13110–13117. http://dx.doi.org/10.1523/JNEUROSCI.2569-11.2011